Schottky diodes with high series resistance: Limitations of forward *I-V* methods

V. Aubry and F. Meyer
Institut d'Electronique Fondamentale, URA CNRS 22, Université Paris Sud, 91405 Orsay Cedex, France

(Received 21 January 1994; accepted for publication 6 September 1994)

Some methods have been proposed to deduce the value of Schottky parameters from forward *I-V* characteristic even in the presence of a large series resistance. In this paper, some well-known methods have been applied to experimental data of a real diode and to computer calculated curves. A comparison is made between these methods and the standard procedure. Some indications are given on the validity and the main limitations of all these techniques. © *1994 American Institute of Physics.*

I. INTRODUCTION

For many years, the metal-semiconductor contact system has been the subject of many investigations, because of its presence in electronic circuits, its importance in advanced VLSI or ULSI technologies, and its fundamental interest to understand the formation of a Schottky barrier.

The parameters, which characterize such a contact, are often determined with difficulty, their values depend on the method used, and must be considered with care. Generally, current-voltage measurements (*I-V*) or capacitance-voltage characteristics $(C\text{-}V)^{1-6}$ are used to extract Schottky parameters. Measurement of differential capacitance and plotting $1/C^2$ vs V_{reverse} (with $C=A\epsilon\epsilon_0/W$, A the diode area, and W the depletion width) are used to obtain V_{bi}, the diffusion potential, by extrapolating to $1/C^2=0$. The barrier height is $\Phi_{bn}=qV_{bi}+(E_c-E_F)$ for a n-type semiconductor.[1–5] *I-V* measurements are also used in order to determine Φ_b and the conduction mode across the metal-semiconductor interface.[1–5] The behavior of a real Schottky diode can be modeled by the equivalent electrical circuit shown in Fig. 1. A series resistance R_s is associated with the bulk material in the semiconductor and the ohmic back contact. G_p is a parallel conductance, which may account for leakage currents. They are both independent of the applied voltage. Then, the relationship between the current I and the voltage drop across the junction V_d is usually given by the following equation:

$$I=I_s\left(\exp\frac{\beta V_d}{n}-1\right)+G_pV_d, \tag{1}$$

where $\beta=q/kT$, I_s the saturation current, and n the ideality factor.

Taking into account the series resistance R_s, Eq. (1) becomes

$$I=I_s\left[\exp\frac{\beta(V-R_sI)}{n}-1\right]+G_p(V-R_sI), \tag{2}$$

with V the applied voltage.

The effect of G_p is more important for diodes with high barrier height and on the reverse bias characteristics. Moreover, Werner[6] showed that the correction of the forward current I for the shunt current does not influence the determination of the different parameters of diodes with the Schottky barrier as high as 0.830 eV. Therefore, G_p will be neglected.

With $G_p=0$, the current I is given as follows:

$$\text{under a reverse bias, } I\approx I_s, \tag{3}$$

$$\text{under a forward bias, } I=I_s\left[\exp\frac{\beta(V-R_sI)}{n}-1\right]. \tag{4}$$

I_s can be determined from Eq. (3) or (4).

The saturation current is usually described within the thermionic emission theory:

$$I_s=A^*AT^2\exp\left(\frac{-\Phi_b}{kT}\right). \tag{5}$$

A^* is the Richardson constant and A the area of the diode. Assuming A^* and Φ_b to be nearly constant, Φ_b is deduced from Eq. (5). The ideality factor n in Eq. (4) is equal to 1 and the thermionic current is

$$I_{\text{th}}=A^*AT^2\exp\left(\frac{-\Phi_b}{kT}\right)\left(\exp\frac{qV_d}{kT}-1\right). \tag{6}$$

A more rigorous analysis of the thermionic current should include the voltage dependence of Φ_b and should take onto account image force lowering and field-induced barrier lowering,[2] in particular.

The assumption $n=1$ may be inappropriate for several reasons:

(1) It can be affected (increased) by image force lowering and the presence of interface states.[1–3] Nevertheless, if the transport current is due to thermionic mechanism, expression (5) is still valid, but with $n>1$.

(2) A mode of carrier transport other than thermionic emission might dominate. Depending on doping levels, temperature, and barrier height, the current transport mechanism takes shapes[1–5] other than the thermionic one:

a. The generation-recombination current.[2] This originates in the space charge region W:

$$I_{\text{gr}}=A\frac{qn_iW}{2\tau}\left[\exp\left(\frac{qV_d}{2kT}\right)-1\right], \tag{7}$$

where n_i is the intrinsic carrier concentration, W the depletion width, which varies with V_d, and τ denotes the effective carrier lifetime. The ideality factor is equal to 2 in this case.

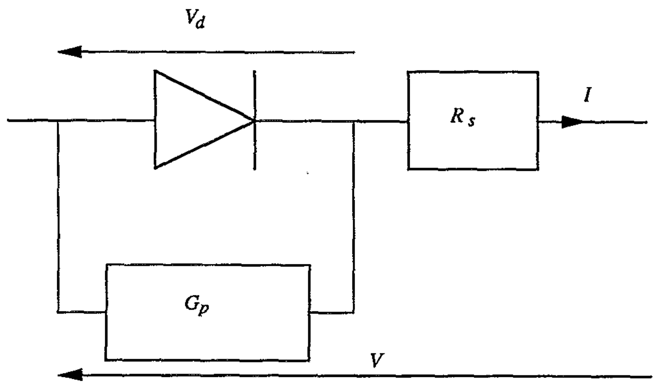

FIG. 1. Equivalent circuit of a real Schottky diode, with a series resistance R_s and a parallel conductance G_p.

Generally, the thermionic current is accompanied by the generation-recombination current. A comparison with Eq. (6) shows that the ratio I_{gr}/I_{th} decreases with increasing forward voltages. The contribution of the both currents yields the more complicated equation:

$$I = A^* A T^2 \exp\left(-\frac{\Phi_b}{kT}\right)\left[\exp\left(\frac{qV_d}{kT}\right)-1\right] + A\,\frac{qn_i W}{2\tau}\left[\exp\left(\frac{qV_d}{2kT}\right)-1\right]. \quad (8)$$

b. Tunneling across the interface.[2] The I-V characteristics at moderate values of voltage have the form

$$I_{tu} = I_s\left\{\exp\left[\frac{qV_d}{E_{00}\coth\left(\frac{E_{00}}{kT}\right)}\right]-1\right\}, \quad (9)$$

where E_{00} and I_s are functions of T, Φ_b, and parameters of the semiconductor. For low temperatures, where $kT/E_{00}<1$, field-emission tunneling is expected. At high temperatures, $kT/E_{00}>1$ and thermionic field emission occurs. The ideality factor n is usually greater than 1.

c. The injection of minority carriers into the semiconductor. This is another possible transport mechanism and it affects the current at high forward voltages.

(3) Finally, $n>1$ can be the result of barrier inhomogeneities at the Schottky contact.[7]

Despite these possible complications, the I-V characteristic of a real diode is often described within the thermionic emission theory regardless of the n value. Consequently, the barrier height Φ_b, determined from Eq. (5), is only the result of a calculation, and has no real physical meaning if the thermionic current ($n=1$) is not the dominant regime. An accurate determination of Schottky parameters is therefore required to understand the behavior of the interface and to correctly model the transport properties of the Schottky barrier.

Several methods have been proposed to extract the different parameters of Schottky diodes,[6,8–17] but few attempts[9,16] have been made to compare the parameter values obtained from these different techniques.

The present paper compares the limitations of different methods which use I-V curves to determine the parameters of Schottky diodes with high series resistance.

The paper is organized as follows. In Sec. II, we present several well established methods that determine the parameters from forward I-V characteristics. These different methods are applied to an experimental curve in Sec. III and to computer calculated curves in Sec. IV. We try to compare these different methods to determine their limitations and finally to establish some user's rules in order to get the most reliable and accurate evaluation of R_s, n, and Φ_b.

II. FORWARD BIAS *I-V* METHODS

The first idea is to fit the experimental I-V curve with Eqs. (4) and (5) where the three fit parameters are R_s, n, and Φ_b. This model fails when n is voltage dependent.[6] Donoval *et al.*[8] chose the case where deviation of n from 1 is caused by a recombination current contribution and by the influence of a series resistance [Eq. (8)]. These effects are introduced into a computer in order to fit the experimental forward I-V data. The difficulty is to find the good values of R_s, n, Φ_b, and τ that well fit $\ln I$ vs V with a minimum of deviation. More recently, Evangelou *et al.*[9] have used the Merlin-multidimensional minimization system program to analyze the I-V characteristics of Schottky diodes. The I-V characteristics are described with Eq. (1) by taking into account a series resistance R_s and a shunt resistance $R_p (R_p = 1/G_p)$. Both of these techniques suffer from the fact that they do not give any indication on the validity of the model used to describe the current transport. In addition, Werner[6] showed that numerical agreement between measured and fitted I-V data is not sufficient to ensure the validity of a model.

Other methods have been developed to extract the values of R_s, n, and Φ_b. The hypotheses of these methods are: (1) Φ_b is determined from Eq. (5) even if $n \geqslant 1$, (2) Φ_b and n are voltage independent, and (3) Eq. (4) is approximated for $V_d = V - R_s I \gg nkT/q$, and becomes:

$$I = A^* A T^2 \exp\left(-\frac{\Phi_b}{kT}\right)\exp\frac{q(V-R_s I)}{nkT}. \quad (10)$$

Equation (10) predicts a linear variation of $\ln I$ vs V_d:

$$\ln I = \ln I_s + \frac{qV_d}{nkT} = \ln I_s + \frac{q(V-R_s I)}{nkT}. \quad (11)$$

The plot $\ln I$ vs V remains a straight line as long as $V \gg nkT/q$ and $V \gg R_s I$. This plot is used in the standard method,[1–5] I_s is extrapolated from the intercept with the zero voltage axis, and the zero voltage barrier height Φ_b is deduced from Eq. (5). As R_s increases, this linear region shrinks. For high series resistance, Norde,[10] Lien *et al.*,[11] and Werner[6] have developed other methods.

A. Standard forward *I-V* method

The principle is to force the I-V data[1–5] to agree with Eq. (10). The parameters are R_s, n, and Φ_b. In our case, we proceed by iterative calculations as follow. For values of the

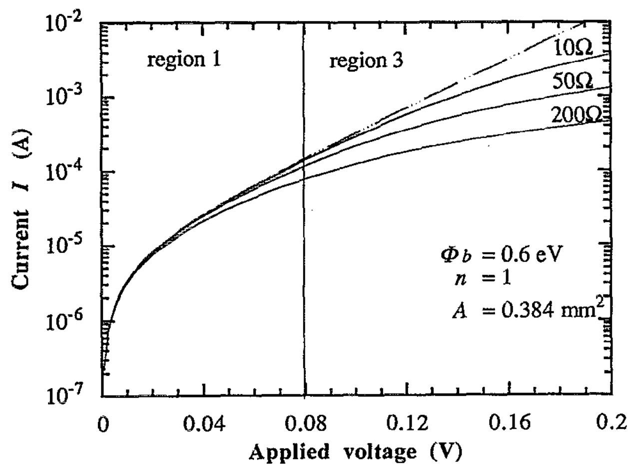

FIG. 2. I-V curves for a Schottky barrier diode with series resistance (full lines) R_s=10, 50, and 100 Ω and the linear extrapolation (dotted line) for Φ_b=0.60 eV, n=1 and A=0.384 mm^2.

series resistance R_s, a computer program corrects the experimental curve $\ln I$ vs V, which becomes $\ln I$ vs $V_d=V-R_sI$. Then, a least-square fit is made over a voltage range (V_{d1},V_{d2}) as wide as possible. A correlation coefficient ρ is calculated in order to quantify the linearity of $\ln I$ vs V_d. The best fit ($\rho=\rho_{\max}$) gives I_s and Φ_b from the intercept with the y axis and n is deduced from the slope. Difficulties arise for highly resistive diodes when the measured curve $\ln I$ vs V shows no linear regime (Fig. 2) between region 1($V<3kT/q$), where a nonexponential behavior is observed, and region 3, where the curve is strongly affected by the voltage drop across the series resistance. Other methods must be introduced to evaluate the barrier height and the ideality factor, as well as the series resistance. These methods often use plots of auxiliary functions and are now described.

B. Norde method

Equation (10) is used while the Schottky diode is assumed to be ideal, namely with $n=1$. Norde[10] has proposed a new technique based on an auxiliary function:

$$F(V,I)=\frac{V}{2}-\frac{kT}{q}\ln\left(\frac{I}{A^*AT^2}\right)=-\frac{V}{2}+\frac{\Phi_b}{q}+R_sI. \quad (12)$$

By plotting F vs V and F vs I, one finds a minimum $F(V_0,I_0)$, which is the point of interest.

From the value of $F(V_0,I_0)$ and the corresponding current I_0 at the minimum, the barrier height and the series resistance can be obtained:

$$I_0=\frac{kT}{qR_s},$$

$$\Phi_b=qF(V_0,I_0)+\frac{qV_0}{2}-kT. \quad (13)$$

The differential conductance of an ideal diode $G_d=dI/dV_d=qI/kT$ can be defined for each point of the I-V curve. It is to be noted that $G_d(I_0)=dI/dV_d=1/R_s$ at the minimum point of $F(V)$.

The disadvantages of this method are that: (1) The ideality factor n is assumed to be unity, which is not always true for a real diode; (2) a single point (V_0,I_0), corresponding to the minimum, is used to calculate the barrier height.

Sato *et al.*[12] tried to improve this method by using $F(V,I)$ at two different temperatures (129 and 297 K). They showed that Φ_b, n, and R_s can be determined even if $1<n<2$. However, they assumed that n does not depend on temperature. However, a dependence of n on T is often observed. For example, Padovani and Sumner[18] found that n increases with decreasing temperature. Their data on Au-n-GaAs diodes could be fitted in terms of the empirical equation $n=T_0/T+1$, where $T_0\approx46$ K. Hackan and Harrop[19] also carried out detailed measurements of I-V characteristics of Ni-n-GaAs diodes as a function of temperature. Their results showed that T_0 is not a constant and that the temperature dependence of n is of the type $n=(\alpha/\sqrt{T})+\beta$, where α and β are constants. Moreover, Aboelfotoh[20] showed that the barrier height of W or WSi_2 onto n-type silicon is affected by the temperature. In conclusion, the method of Sato *et al.*[12] can only be used if it has been checked that the Schottky parameters do not depend on T. Finally, the current contribution due to recombination is strongly enhanced at low temperatures. Such an effect clearly appears on the low-temperature I-V characteristic reported by Sato *et al.*[12] but was completely ignored by these authors. A similar approach was proposed by Manifacier *et al.*[13] These authors used the simple function $F(I)=V-R_0I$. The maximum values, $F(I_M)$, for two different values of the parameter R_0 lead to the determination of R_s, n, and Φ_b.

C. Lien, So, and Nicolet method

This method[11] is based on plotting several Norde-type functions defined by

$$G_\gamma(V,I)=\frac{V}{\gamma}-\frac{kT}{q}\ln\left(\frac{I}{A^*AT^2}\right), \quad (14)$$

where γ is an arbitrary parameter greater than n. It is to be noted that for $\gamma=2$, $G_2(V,I)=F(V,I)$, and the Norde plot is obtained.

Plots of $G_\gamma(V,I)$ vs I show a minimum for $I_{0\gamma}=(kT/qR_s)(\gamma-n)$. The plot of $I_{0\gamma}$ vs γ is a straight line whose slope leads to the value of the series resistance R_s, and whose extrapolated intercept at $I_{0\gamma}=0$ gives n. The advantage of using a set of different values of γ, instead of only one in the Norde plot, resides in the fact that several data points of the I-V characteristic are used. A linear regression can be performed to calculate R_s, which raises the accuracy of the results. The ideality factor is no more supposed to be equal to unity. In Appendix A, it is shown that the differential conductances $G=dI/dV$ and $G_d=dI/dV_d$ of the real ($R_s\neq0$) and ideal ($R_s=0$) diodes are simply related to the series resistance R_s at the minimum point of the auxiliary functions by $G(I_{0\gamma})R_s=(\gamma-n)/\gamma$ and $G_d(I_{0\gamma})R_s=(\gamma-n)/n$. As a variant of their technique, Lien *et al.*[11] suggested plotting $I_{0\gamma}$ as a function of $(d \ln I/dV)^{-1}$, which is similar to $I_{0\gamma}$ vs γ. Indeed, differentiating Eq. (14) and setting $dG_\gamma/dV=0$ at some current $I_{0\gamma}$ demonstrate that $\gamma=1/\beta\ (d \ln I/dV)$. This procedure has the advantage of eliminating the explicit evaluation of a set of functions $G_\gamma(V,I)$ and is easy to carry out with computer controlled I-V measurements.

Bohlin[14] only used two different values of γ and obtained a set of two equations similar to Eq. (13) that he had to solve. However, he only used two values of γ and thus two experimental data points.

It is to be noted that Cibils and Buitrago[15] proposed another approach to generalize the Norde method. They used a voltage as the arbitrary parameter instead of the dimensionless parameter γ. All these last methods (Secs. II B and II C) involve the determination of the minimum of an auxiliary function, which may lead to some uncertainties. Very recently, Lee *et al.*[16] have proposed a new approach, which involves the use of the auxiliary function suggested by Cibils and Buitrago[15] and a computer fitting routine. This method avoids the uncertainties due to the determination of a minimum.

D. Werner method

Werner[6] has proposed examining three different plots for the determination of I_s, Φ_b, n, and R_s from I-V characteristics. One of the three plots, the so-called plot C was previously used by Cheung and Cheung[17] and is very similar to the variant technique proposed by Lien *et al.*,[11] but Werner[6] showed that the first plot, called plot A, gave the most reliable and accurate values for R_s, Φ_b, and n. In the following, we will only consider the so-called plot A.

Under forward bias, for $V_d=V-R_sI \gg (nkT)/q$, current I is given by Eq. (10) and this equation yields for the differential conductance $G=dI/dV$ of the real diode:

$$\frac{G}{I}=\frac{\beta}{n}(1-GR_s). \qquad (15)$$

Equation (15) shows that a plot of G/I vs G yields a straight line that leads to $1/R_s$ and β/n from the x- and y-axis intercepts, respectively. G can be determined either experimentally or numerically. In this last case, to limit the effect of noise on the differential conductance, it is important to use several data points to calculate the derivative of the measured I-V characteristics.

The last methods do not yield directly the value of Φ_b. As proposed by Werner,[6] the series resistance determined by these methods can be introduced to correct the voltage axis of the I-V curve. Then n and Φ_b can be evaluated from the corrected curve I-V_d by using the standard forward method.

In order to overview the problems, the next paragraph will deal with an experimental curve I-V whose parameters will be determined by four typical methods described above: the standard technique and the methods proposed by Norde,[10] Lien *et al.*,[11] and Werner.[6]

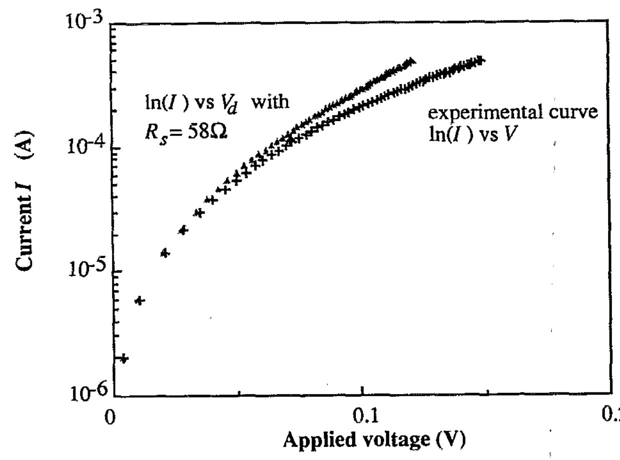

FIG. 3. Experimental forward I-V characteristic of a Schottky diode W/n-Si, plotted on a semilogarithmic graph. The corrected curve, corresponding to R_s=58 Ω (see Table I), is also plotted.

III. STUDY OF AN EXPERIMENTAL CURVE

The samples are prepared as follows. The Si surface was cleaned by using a standard chemical cleaning procedure, including a final dip in diluted HF. W films were deposited by dc magnetron sputtering on a 1 Ω cm n (100)-oriented Si wafer. For I-V measurements, patterns with different areas were defined by conventional photolithography.

The different techniques have been applied to an experimental I-V characteristic obtained for a 0.384 mm^2 area diode (Fig. 3). The results directly deduced from these analyses are reported in Table I. The standard method is used in the range $(V_{d1},V_{d2})=0.09$–0.12 V in order to satisfy the condition $V_d > (3nkT)/q$. The correlation coefficients ρ vs R_s have a maximum, which should theoretically correspond to the best fit (Fig. 4). However, this value of R_s is not high enough to give a linear $\ln I$ vs V_d curve (Fig. 3). The plots of the auxiliary functions corresponding to the other methods are reported on Figs. 5(a)–5(c). The Norde plot obviously yields a too high value for R_s as shown in Fig. 6(a). The series resistances deduced from the plots of Lien *et al.* and Werner are very similar and lead to nice linear $\ln I$ vs V_d curves [Fig. 6(b)]. These values of R_s were introduced for standard treatment of the I-V characteristic to determine Φ_b and n. The results are indicated in Table II and correspond to

TABLE I. Direct determination of R_s, n, and Φ_b by using the standard and Norde methods. Lien *et al.* and Werner plots indicate that these methods do not directly yield the barrier height.

Methods	R_s (Ω)	Φ_b (eV)	n
Standard[a]	58	0.55	1.52
Norde[b]	112	0.57	1 (hypothesis)
Lien *et al.*[c]	72		1.34
Werner[d]	68		1.37

[a]See Refs. 1–5.
[b]See Ref. 10.
[c]See Ref. 11.
[d]See Ref. 6.

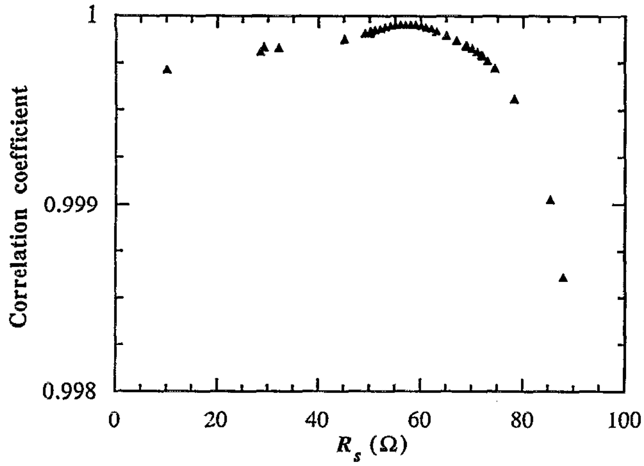

FIG. 4. Correlation coefficient ρ vs R_s in the range 0.09–0.12 V. The maximum $R_s \approx 58\ \Omega$ is used to correct the experimental curve in Fig. 3.

rather good correlation coefficients and similar values of Φ_b. Nevertheless, a large discrepancy is observed on n, 1.29 against 1.38.

To summarize, some features can be deduced from these results: (a) the ideality factor seems to be very sensitive to R_s and is obviously high in this case; (b) as expected, the Norde method fails when n differs from 1; (c) the other methods lead to the same barrier height.

At this point, our discussion suffers from the fact that we are unable to determine which technique gives the results closest to the true values. To have a better knowledge of these methods and their limitations, a program of simulated Schottky diodes I-V characteristics has been developed.

IV. LIMITS OF THE FORWARD I-V METHODS

It is possible within this program written in BASIC to take into account:

(1) the characteristics of the diode: semiconductor, type, doping concentration, area, parallel conductance, series resistance, and barrier height, and

(2) the conduction mode, by using Eqs. (6) and (7) for thermionic and generation-recombination mode. For the other conduction modes, the general Eq. (4) is used and I_s is obtained according to Eq. (5), where Φ_b is an apparent barrier.

(3) It is possible to take into account several conduction modes simultaneously.

(4) In addition, the program does not neglect the image force lowering $\Delta\Phi$ in its calculations[1–3] even if this effect is more pronounced for large reverse bias.[1–5] The expression[2] used for $\Delta\Phi$ is $\{[q^3 N_d(V_{bi}-V_d)]/[8\pi^2(\epsilon_0\epsilon)^3]\}^{1/4}$. It is important to note that the effect of the image force lowering still exists at the zero voltage condition, but does not exist any longer at the flatband condition.[2]

These simulations evidence the influence of the conduction modes and the series resistance on I-V characteristics. The calculated characteristics can be used as experimental data to compare the performance of the different techniques in evaluating the Schottky parameters. The limitations of each method must be due, first of all, to unsatisfied hypotheses: $n(V)$ and $\Phi_b(V)$ are not constant and $V_d \gg (nkT)/q$ is not respected, for example. Moreover, the sensitivity of each

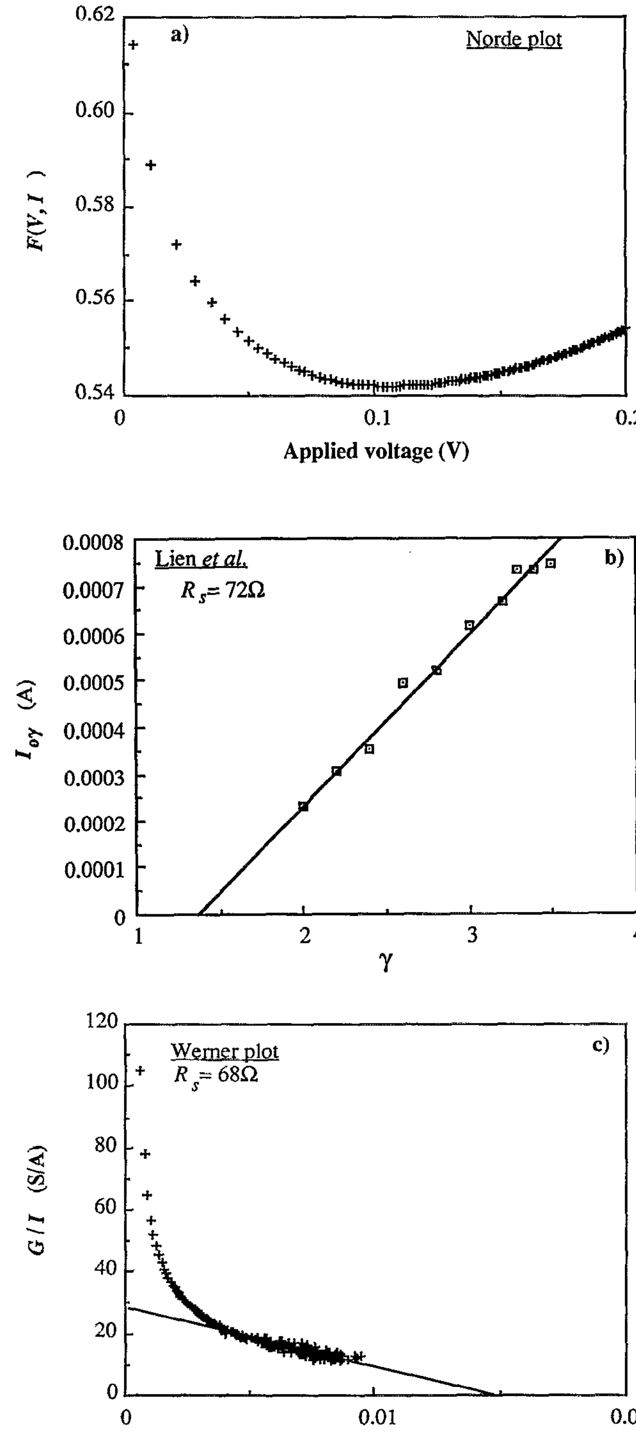

FIG. 5. (a) Norde plot of $F(V,I)$ for the Schottky diode W/n-Si; the minimum point gives $R_s \approx 112\ \Omega$. (b) I_0 [Lien *et al.* (Ref. 11)] obtained from the minimum of G_γ, are plotted against γ and lead to R_s is 72 Ω. (c) Data from Werner method: G/I vs G; $R_s = 68\ \Omega$ are evaluated from the x-axis intercept.

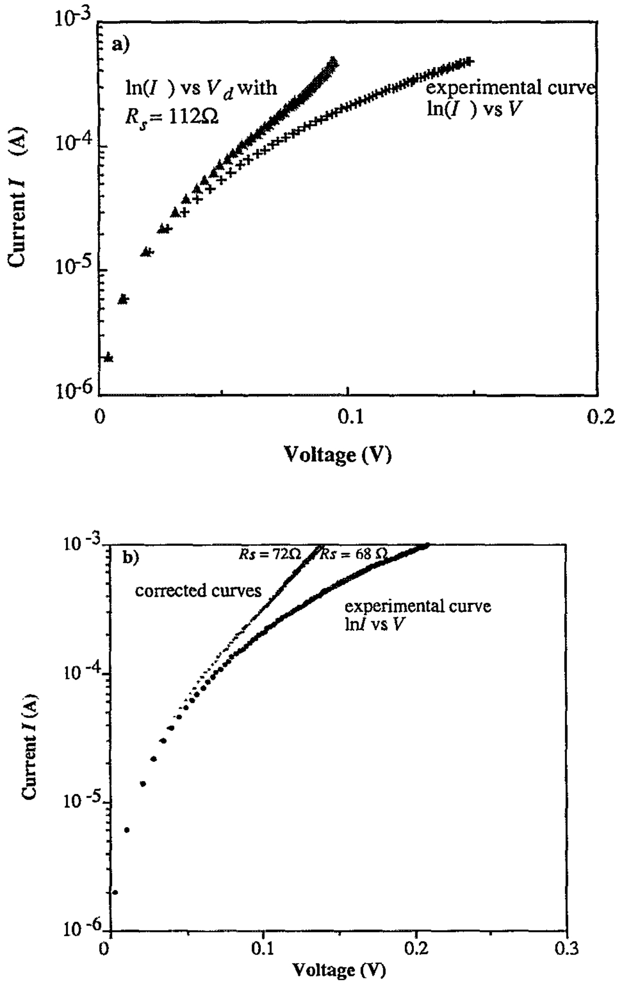

FIG. 6. Plots of the experimental curve and the corrected curves with (a) R_s=112 Ω, and (b) R_s=72 and 68 Ω.

method to the series resistance or to the current step used (or voltage step) may differ. Four different simulations have been performed. For all the simulations, the barrier height was 0.60 eV; semiconductor was n type with a doping concentration of 10^{16} atoms/cm^3 and a Richardson constant of 112 A cm^{-2} K^{-2}. The area of the diode was that of the sample described above, 0.384 mm^2. The series resistance

TABLE II. Parameters of the experimental curve determined by the four different methods. R_s is calculated directly by the standard method and from the plots of the three other methods. Φ_b and n are then determined by using the semilogarithmic delineation after correcting the curve for the voltage drop due to R_s. The correlation coefficient ρ is calculated in the range 0.09–0.12 V.

	R_s (Ω)	Φ_b (eV)	n	ρ
Standard method	58	0.55	1.52	0.999 952
Norde[a]	112	impossible	impossible	
Lien *et al.*[b]	72	0.55	1.29	0.999 78
Werner[c]	68	0.55	1.38	0.999 84

[a]See Ref. 10.
[b]See Ref. 11.
[c]See Ref. 6.

TABLE III. Simulations of different conduction modes in a Schottky diode metal/n-Si with Φ_b=0.60 eV, R_s=50 Ω, A=0.384 mm^2, and A^*=112 A cm^{-2} K^{-2}.

Conduction mode	Other parameter
(a) Pure thermionic	n=1
(b) Thermionic and generation-recombination	τ=1 μs
(c) Thermionic and generation-recombination	τ=10 ps
(d) Other regime	n=1.2

had a classical value of 50 Ω. The four types of conduction mode were (1) pure thermionic emission [Eq. (6)], (2) both thermionic emission and generation-recombination emission with τ=1 μs, and (3) τ=10 ps [Eq. (8)]; other emissions where n=1.2 (see Table III). As it is shown in Fig. 7, when τ=1 μs the recombination current is too small to have any influence on the total current. This is no longer the case when τ=10 ps. Of course, this last value is very low, and has only been observed in poor quality heteroepitaxial films.[21] We have nevertheless considered this case as very similar effects should be observed on diodes with better carrier lifetimes and higher values of Φ_b.

A. Standard method

The main problems lie in the choice of the voltage range (V_1, V_2) over which ln I-V is linear. The external voltage V differs from the voltage $V_d = V - R_s I$ applied to the junction. The lower voltage V_1 must be large enough to satisfy the condition $V_1 - R_s I_1 = V_{d1} \gg (nkT)/q$, and, in addition, the correction $R_s I_1$ must remain limited.

1. Range (V_{d1}, V_{d2})

For calculated I-V characteristics, the series resistance is not a limiting parameter. The correlation parameter does

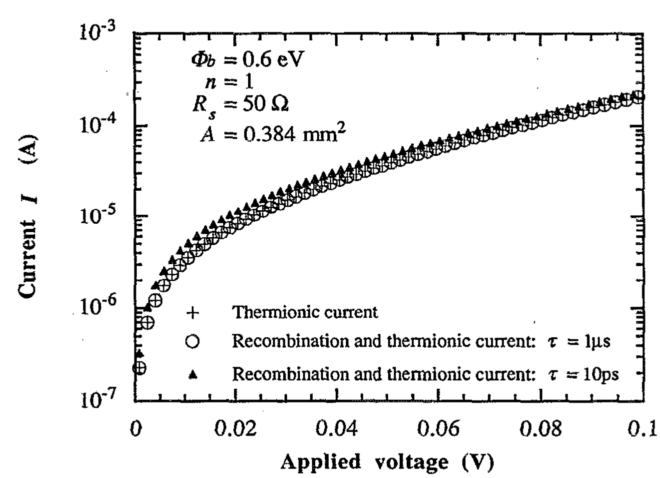

FIG. 7. I-V curves simulated with Φ_b=0.60 eV, R_s=0 Ω. (a) thermionic conduction (cross) and (b) thermionic+generation-recombination with τ=1 μs (open circle) or τ=10 ps (full triangle).

TABLE IV. Ranges (V_{d1}, V_{d2}) used to study the different curves. The correspondent values of V_1 and V_2 for three conduction modes (pure thermionic emission, both thermionic emission and generation-recombination with τ=10 ps, and other regime with n=1.2) are also reported.

			V_1 (V)/V_2 (V)		
Range	V_{d1} (V)	V_{d2} (V)	Pure thermionic	Thermionic and recombination with t=10 ps	Other regime
1	0.0775	0.12	0.084/0.155	0.085/0.158	0.081/0.136
2	0.09	0.12	0.101/0.155	0.103/0.158	0.083/0.136
3	0.20	0.24	0.950/3.54	0.950/3.54	0.400/0.940

reach its maximum value for the good value of R_s unless n is not a constant, V_d is not large enough with respect to $(nkT)/q$, or, finally, if the image force lowering is not taken into account during the data processing.

Three different voltage ranges have been chosen (Table IV). Ranges 1 and 2 give indications on the validity of the often assumed condition $V_d \geqslant (3kT)/q$ and on the influence of a generation-recombination current. We have arbitrarily chosen another range (range 3) with high values of V_{d1} and V_{d2} although it leads to a high and unrealistic applied voltage range (V_1, V_2). This range must correspond to an exponential behavior of the I-V_d characteristic and may evidence the effects on n and Φ_b when the image force lowering is not taken into account during data processing.

The study of the curves was performed with a scan of 1 Ω for R_s. The values indicated in Table V correspond to the maximum of the correlation coefficient ρ. When n is a constant (n=1 or n=1.2), the use of low-voltage ranges (ranges 1 and 2) always underestimates the ideality factor, while n is overestimated over range 3 (Table V). The failure for low voltages clearly demonstrates that the condition $V_d \geqslant (3kT)/q$ and the usual assumed condition $V \geqslant (3kT)/q$ are not restrictive enough. The n overestimate and the barrier height underestimate for high voltages can be explained by the fact that the image force effect is not taken into account during data processing. As had been indicated earlier, the image force lowering under zero voltage condition ($\Delta\Phi$ =0.02 eV) must be added to the zero voltage barrier determined from I-V characteristics to recover the barrier at the flatband condition, which is introduced in the simulations.

As expected, a generation-recombination current results in an increase of n, rather pronounced for low voltages and even efficient over range 3.

TABLE V. Determination of the parameters for the four simulations depending on the range used.

Diode parameters	Range 1	Range 2	Range 3
Pure thermionic current Φ_b=0.60 eV R_s=50 Ω	R_s=52±1 Ω n=0.96 Φ_b=0.58 eV	R_s=50±1 Ω n=0.98 Φ_b=0.58 eV	$R_s \approx$50±1 Ω $n \approx$1.02 Φ_b=0.58 eV
Thermionic current Φ_b=0.60 eV R_s=50 Ω and recombination current with τ=1 μs	R_s=52±1 Ω n=0.96 Φ_b=0.58 eV	R_s=51±1 Ω n=0.98 Φ_b=0.58 eV	$R_s \approx$50±1 Ω $n \approx$1.02 Φ_b=0.58 eV
Thermionic current Φ_b=0.60 eV R_s=50 Ω and recombination current with τ=10 ps	R_s=50±1 Ω n=1.06±0.02 Φ_b=0.57 eV	R_s=50±1 Ω n=1.06±0.02 Φ_b=0.57 eV	$R_s \approx$50±1 Ω $n \approx$1.03 Φ_b=0.57 eV
Other regimes "Φ_b=0.60 eV" R_s=50 Ω n=1.2	R_s=50±1 Ω n=1.16 Φ_b=0.58 eV	R_s=50±1 Ω n=1.17 Φ_b=0.58 eV	R_s=50±1 Ω n=1.23 Φ_b=0.58 eV

2. Limitation due to series resistance

For real Schottky diodes, noise and measurement uncertainty distort the I-V characteristics.[9] The maximum of the correlation coefficient does not indicate then the correct value of the series resistance (see Sec. III).

Thus the diode parameters can only be determined if the $\ln I$-V plot shows a straight-line part over a voltage range large enough. We can assume that this voltage interval is too small when R_s is larger than a value given by $R_{s\max} I_1 \approx V_{d1}/100$. This maximum value $R_{s\max}$ is plotted as a function of the barrier height in Fig. 8. With Φ_b=0.60 eV, for example, R_s must be smaller than 5 Ω to observe a linear portion on the $\ln I$-V plot (see Fig. 2). For larger series resistance, the correction of the I-V curve must be performed by using the plots of auxiliary functions proposed by Norde,[10] Lien *et al.*,[11] or Werner.[6]

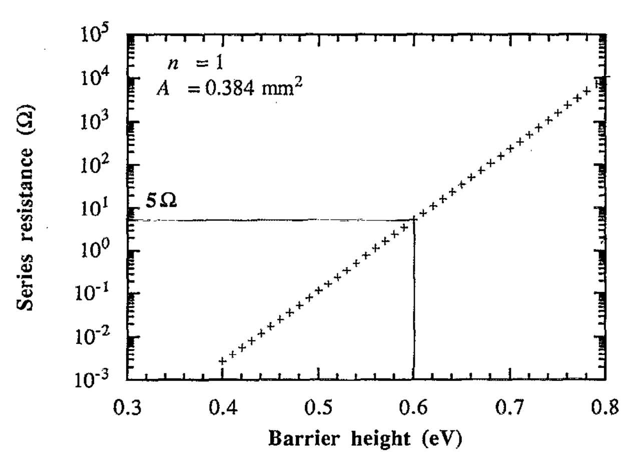

FIG. 8. Plot of R_s vs Φ_b when $R_s I = V_{d1}/100$, i.e., plot of the maximum value of R_s which allows a linear region of ln(I) vs V.

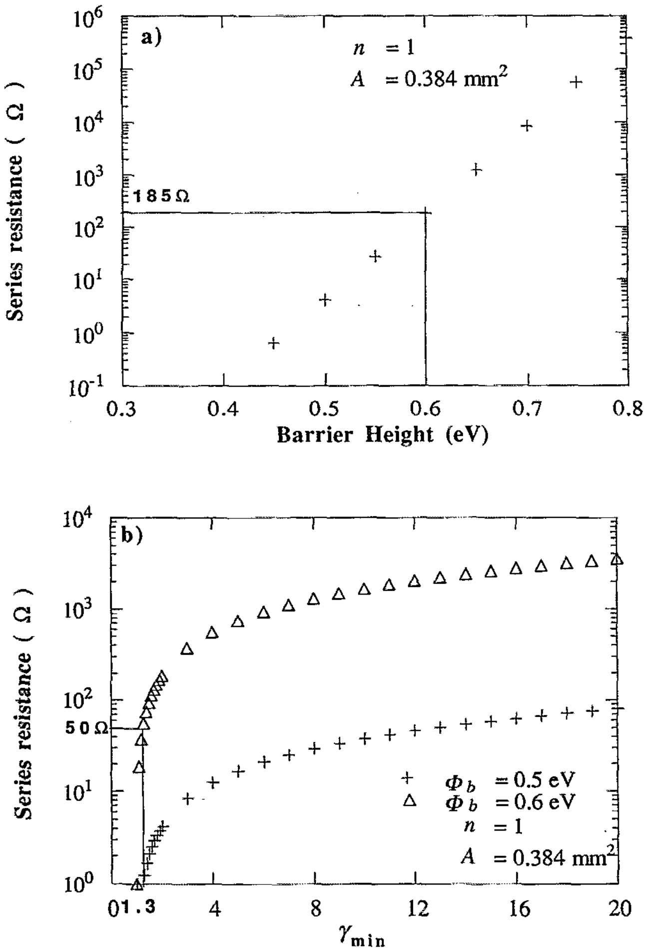

FIG. 9. In the case of $n=1$, (a) R_s vs Φ_b to satisfy to the condition $V_{d0}>(3kT)/q$ for the Norde method and (b) R_s vs γ to satisfy the condition for the Lien *et al.* method.

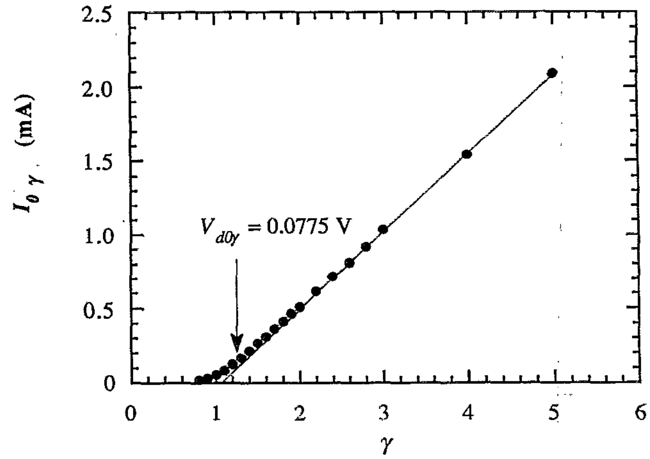

FIG. 10. Plot of $I_{0\gamma}$ vs γ for $n=1$, $\Phi_b=0.60$ eV and $R_s=50$ Ω. This plot is linear for $\gamma\geqslant 1.3$.

B. Methods of Norde and Lien *et al.*

Both methods are based on the seeking of function minimum. The method developed by Norde[10] uses only one data point to calculate Φ_b, whereas that proposed by Lien *et al.*[11] uses several data of the I-V characteristic. The Norde method was originally not intended for nonideal diodes with $n>1$, and Lien *et al.* proposed a way to remedy this difficulty. Meanwhile, the disadvantages of these both methods are that (1) the I-V characteristic is approximated by Eq. (11), (2) they are based on the accurate determination of a minima, and (3) n is assumed not to depend on V.

1. Voltage range

The use of Eq. (11) implies that the voltage across the diode V_{d0}, corresponding to the minimum, fulfills the condition $V_{d0}\geqslant n(kT/q)$. A relation between R_s and Φ_b may be found in order to meet the condition $V_{d0}\geqslant 3n(kT/q)$ for the minimum of the functions used by Norde[10] and by Lien *et al.*[11] These conditions on R_s are plotted in Figs. 9(a) and 9(b). When $n=1$ and $\Phi_b=0.60$ eV, Fig. 9(a) shows that the minimum of $F(V,I)$ will satisfy $V_{d0}>(3kT)/q$, provided that R_s does not exceed the value of 185 Ω. Remember that for the standard method, the linear region disappears completely for values as low as $R_s=5$ Ω (see Sec. IV A 2). The Lien *et al.* method[11] offers the possibility to work with even higher values of R_s by increasing the γ values [Fig. 9(b)]. When $R_s=50$ Ω, from Fig. 9(b) it can be deduced that γ must be larger than 1.3. This condition is confirmed by the plot of Fig. 10 where $I_{0\gamma}=f(\gamma)$ clearly shows a nonlinear relationship for $\gamma\leqslant 1.3$. Theoretically, it is possible to increase γ up to the value which corresponds to the maximum power that can be dissipated in the diode, provided that the series resistance is not changed by heating or minority-carrier injection.[6] Moreover, if the voltage drop across the series resistance is larger than the voltage V_d across the diode, the correction on the I-V characteristic is too high to lead to accurate values for the Schottky parameters. Therefore $\gamma_{\min}$ must be limited to about 4 or 5, and R_s must be lower than ≈500 and 20 Ω for $\Phi_b=0.60$ and 0.50 eV, respectively [Fig. 9(b)].

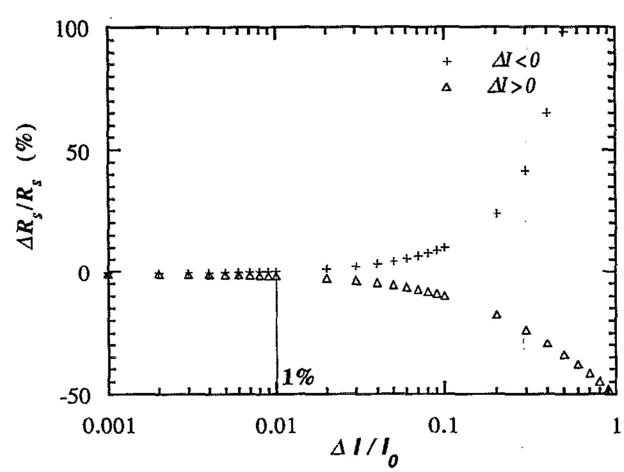

FIG. 11. Plot of the relative error $\Delta R_s/R_s$ vs $\Delta I/I_0$ in the case of $\Phi_b=0.60$ eV, $n=1$, $R_s=50$ Ω.

TABLE VI. Relative error $\Delta R_s/R_s$ obtained with Norde (see Ref. 10) and Lien *et al.* (see Ref. 11) methods, when Φ_b=0.60 eV, R_s=50 Ω, and n=1. The current step ΔI is such as $\Delta I/I$=0.4%.

	Norde	Lien *et al.*
$\frac{\Delta R_s}{R_s}$	0.3%	0.08%

2. Influence of the current step

The determination of minima of $F(I\text{-}V)$ and $G_\gamma(I\text{-}V)$ is subject to error due to the current step ΔI chosen for the data acquisition. In the case of the Norde method, an estimate of this error has been performed.

When the current step is ΔI, the current determined for the minimum is not the real value I_0, but I_0^* which lies between $I_0+\Delta I$ and $I_0-\Delta I$, while $R_s^* = kT/qI_0^*$. The relative error made on the value of R_s is $\Delta R_s/R_s = (R_s^* - R_s)/R_s$. This error increases with $\Delta I/I_0$ (see Fig. 11), and even more when $I_0^* < I_0$. This trend can be explained by the fact that the shape of the curve $F(V,I_0)$. $F(V,I_0)$ varies faster for $I<I_0$ than for $I>I_0$. In order to use the Norde method in good conditions, a small current step is required. From Fig. 11, it seems that $\Delta I/I_0$ must be smaller than 1% to guarantee an accuracy on R_s better than 2%. The method proposed by Lien *et al.*[11] uses several data points and is less sensitive to the current step. This is confirmed by the results reported on Table VI. For $\Delta I/I_0 \approx 0.4\%$, Φ_b=0.60 eV, and R_s=50 Ω, $\Delta R_s/R_s$ is lower than 0.08%.

3. Influence of the conduction mode

We have applied these two methods to $I\text{-}V$ characteristics when n differs from 1. Table VII gives the results. The values of R_s given by the Norde method are too high. The corrected curves (not shown here) are not linear and look like Fig. 6(a). The Norde method fails because the hypothesis n=1 is not valid in these two particular cases. The method proposed by Lien *et al.*[11] leads to better results (Table VII). Meanwhile, it is to be noted that this method is not sensitive enough to the presence of different current contributions and gives a mean value (n=1.03, for instance, for case b, Table VII) over a range of voltage. This weak sensitivity is due to the use of a linear current as an ordinate scale which emphasizes data at high currents but compressed data at low, voltages.

TABLE VII. Norde (see Ref. 10) and Lien *et al.* (see Ref. 11) methods are used, for Φ_b=0.60 eV and R_s=50 Ω and with $\Delta I/I_0 \approx 1\%$, in the two following cases: (1) thermionic current+recombination current with τ=10 (ps) and (2) another regime where n=1.2.

Conduction mode	Norde	Lien *et al.*
(a) n=1.2	$R_s \approx 63$ Ω	$R_s \approx 50.2$ Ω n=1.21 Φ_b=0.58 eV
(b) Thermionic current and recombination current with τ=10 ps	$R_s \approx 53.3$ Ω	R_s=49.9 Ω n=1.03 Φ_b=0.58 eV

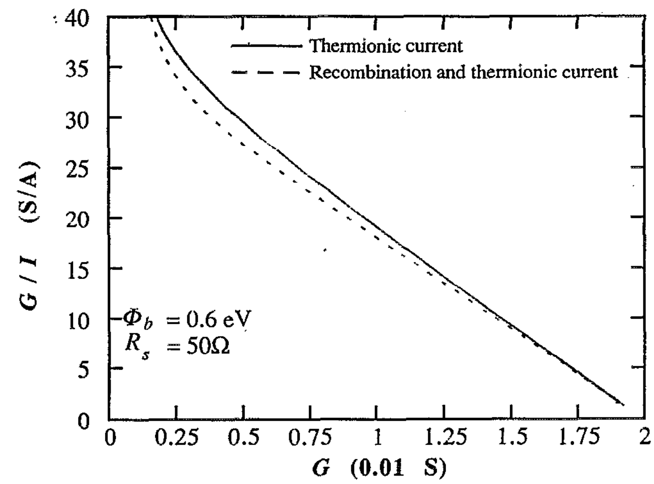

FIG. 12. Plots of G/I vs G with Φ_b=0.60 eV and R_s=50 Ω. The full line corresponds to pure thermionic current; the broken line corresponds to the combination of a thermionic current and a generation-recombination current with τ=10 ps.

C. Werner method

As explained in Sec. II D, the Werner method is based on the plot of G/I vs G, where G is the conductance dI/dV. G can be determined experimentally or numerically. In our case, G was calculated by deriving the $I\text{-}V$ curve with a small voltage step ($\approx$1 mV) to get G more accurately.[6] The effect of noise can be reduced by calculating the derivative of the $I\text{-}V$ characteristic over a small range of data points. Then the detrimental effect observed by Evangelou *et al.*[9] is easily avoided. In this method, $1/R_s$ is the limit of G as G/I tends to 0. The data at the intermediate voltages are emphasized with this technique. Therefore the influence of contributions due to generation-recombination current (low voltages) or minority current (high voltages) is reduced.

1. Sensitivity to the conduction mode

Two curves of G/I vs G, where Φ_b=0.60 eV and R_s=50 Ω, are plotted on Fig. 12. The full line corresponds to the case n=1 and the broken line is that for the combination of a thermionic current and a generation-recombination current (τ=10 ps, case c of Table III). It is to be noted that we observe an increase of G/I as G tends to 0 (Fig. 12). Such a behavior was not reported by Werner;[6] all his plots reach a maximum for a low value of G. Our plots (not shown) indicate the same trend providing that the contribution of a parallel conductance has been taken into account. But this contribution of a parallel conductance has no significant

TABLE VIII. Results by Werner method.

Conduction mode	R_s by Werner	n,Φ_b
Thermionic current	≈50 Ω	n=1.01 Φ_b=0.58 eV
Thermionic current and recombination current with τ=10 ps	≈50 Ω	n=1.03 Φ_b=0.58 eV

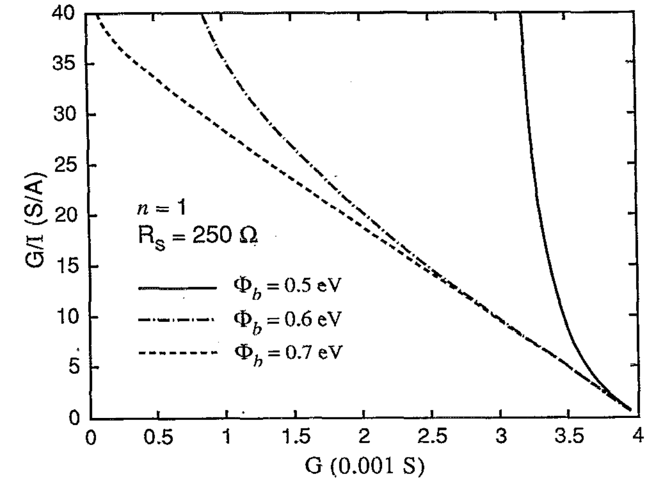

FIG. 13. Plots of G/I vs G, when $n=1$, $R_s=250\ \Omega$, and $\Phi_b=0.50$ (full line), 0.60 (dot and dashed line), and 0.70 eV (broken line).

influence on the determination of R_s. R_s can be easily determined from the x-axis intercept. The R_s value does not depend on the generation-recombination contribution and corresponds to the expected value $R_s=50\ \Omega$ (Table VIII). It is important to note that the influence of a generation-recombination current is well evidenced in the G/I vs G plot (Fig. 12). The Werner method appears to be the most sensitive method to evidence such a contribution.

2. Limitation of the method

Figure 13 shows the influence of the barrier height on Werner plots for diodes with a 250 Ω series resistance. The procedure proposed by Werner[6] leads to the nominal value $R_s=250\ \Omega$ for barrier heights higher than 0.50 eV. When $\Phi_b=0.5$ eV, G/I vs G exhibits no straight-line part and does not allow the extraction of the Schottky parameters. In Appendix A, a relation is derived between G/I and the derivative of the auxiliary function introduced by Lien *et al.*[11] It is shown that the derivative of $G\gamma(V)$, at the minimum point, becomes

$$\frac{dG\gamma(V)}{dV}=\frac{1}{\gamma}-\frac{1}{\beta}\frac{G}{I}=0. \tag{16}$$

It corresponds to particular values of G/I depending on γ:

$$\frac{G}{I}=\frac{\beta}{\gamma}. \tag{17}$$

These values must belong to a linear part of the G/I vs G curve. For example, for $\Phi_b=0.6$ eV, the determination of the Schottky parameters is possible providing γ is chosen larger than 4 ($G/I\leqslant 10\ S/A$), while it will be impossible for $\Phi_b=0.5$ eV (Fig. 13). These results are consistent with those indicated in Fig. 9. In others words, from Eq. (16), one can consider that the method of Lien *et al.*[11] consists of solving $-\beta(dG_\gamma/dV)$ for different γ values as shown in Fig. 14. On this figure, Werner's method can be considered as a limit of the method proposed by Lien *et al.*[11] when γ tends to ∞.

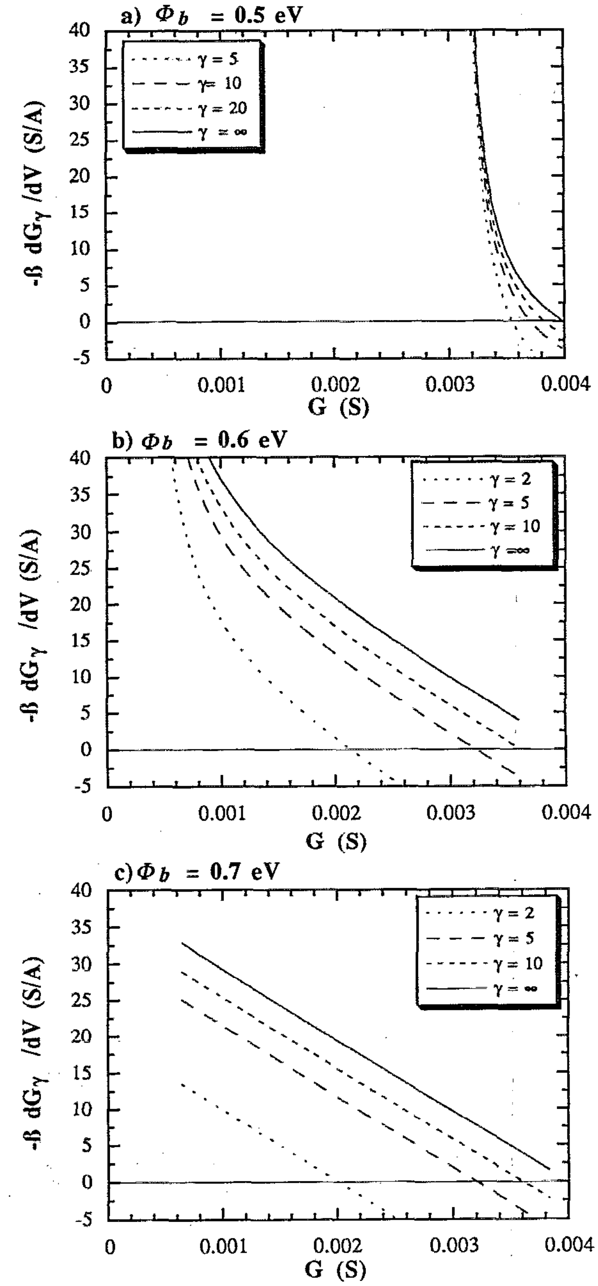

FIG. 14. Plots of $-\beta(dG_\gamma/dV)=(G/I)-(\beta/\gamma)$ vs G for different I-V data represented in Fig. 13 and different γ values. (a) $\Phi_b=0.5$ eV, $\gamma=5$, 10, 20, ∞; (b) $\Phi_b=0.6$ eV, $\gamma=2$, 5, 10, ∞; (c) $\Phi_b=0.7$ eV, $\gamma=2$, 5, 10, ∞.

From this discussion, it clearly appears that the methods introduced by Werner[6] and Lien *et al.*[11] are equivalent mathematically and must lead to the same limitations in terms of barrier height-series resistance.

V. CONCLUSION

Four different methods have been applied to an experimental I-V characteristic and to computer calculated characteristics of Schottky diodes. We have compared the limitations of these four different methods. The standard method is especially limited by the value of the series resistance. The method proposed by Norde[10] leads to some improvements providing that $n=1$. The procedures given by Lien *et al.*[11] and Werner[6] are equivalent mathematically and yield the best results. Their limitations are similar. However, it is to be noted that the Werner approach exhibits some advantages. It appears to be the simplest to use and is obviously the most sensitive method to evidence the contribution of a generation-recombination current In addition, this last method offers the unique advantage to indicate directly, by using a single graph, if the I-V characteristic of the real diode is well described by a purely exponential characteristic in series with a constant resistance.

ACKNOWLEDGMENTS

The authors are grateful to Dr. B. Leroy for fruitful discussions. F. M. also wants to thank her students, Y. Buffet, T. Bourouina, and S. Chapiron for their contributions to this work.

APPENDIX A

The different methods used to extract the Schottky parameters from forward I-V measurements are all based on calculations on $\ln(I)$ and/or $d[\ln(I)]/dV$.

The forward I-V characteristic of a Schottky diode is approximated by

$$I=A^*AT^2 \exp\left(-\frac{\Phi_b}{kT}\right)\exp\frac{q(V-R_sI)}{nkT}. \tag{A1}$$

The function $f(V)=\ln(I/A^*AT^2)$ can be evaluated by

$$f(V)=\beta\frac{V}{n}-\beta\frac{\Phi_b}{q}-\beta\frac{R_sI}{n} \tag{A2}$$

or

$$f(V)=\beta\frac{V_d}{n}-\beta\frac{\Phi_b}{q}, \tag{A3}$$

with $V_d=V-R_sI$.

For the ideal case, $R_s=0$, differentiating Eq. (A2) with respect to voltage gives

$$\frac{df(V)}{dV}=\frac{\beta}{n}. \tag{A4}$$

This relation is used in the standard method to calculate the ideality factor n from the slope of the curve $\ln I$ vs V in a straight part.

For real diode, $R_s\neq0$, differentiating Eq. (A2) now gives a function of R_s and the differential conductance $G=dI/dV$:

$$\frac{df(V)}{dV}=\frac{\beta}{n}-\beta G\frac{R_s}{n}. \tag{A5}$$

By using the identity $(d\ln I/dV)=(1/I)(dI/dV)$, one obtains from Eq. (A5)

$$\frac{df(V)}{dV}=\frac{G}{I}=\frac{\beta}{n}(1-R_sG). \tag{A6}$$

The plot G/I vs G according to Eq. (A6) corresponds to one of the plots introduced by Werner[6] termed plot A.

Moreover, the auxiliary functions proposed by Norde,[10] $F(V)$, and Lien *et al.*,[11] $G_\gamma(V)$, can be written as functions of $f(V)$:

$$F(V)=\frac{V}{2}-\frac{1}{\beta}\ln\frac{I}{AA^*T^2}=\frac{V}{2}-\frac{1}{\beta}f(V), \tag{A7}$$

$$G_\gamma(V)=\frac{V}{\gamma}-\frac{1}{\beta}\ln\frac{I}{AA^*T^2}=\frac{V}{\gamma}-\frac{1}{\beta}f(V), \tag{A8}$$

with γ ranging from n to ∞.

The Norde method[10] can be considered as a particular case, with $n=1$ and $\gamma=2$, of the method proposed by Lien *et al.*[11] One fundamental step of this technique lies in the seeking of the minimum of the auxiliary functions. This minimum, which depends on γ, occurs when

$$\frac{dG_\gamma(V)}{dV}=0,$$

i.e.,

$$\frac{dG_\gamma(V)}{dV}=\frac{1}{\gamma}-\frac{1}{\beta}\frac{df(V)}{dV}=\frac{1}{\gamma}-\frac{1}{n}(1-R_sG)=0. \tag{A9}$$

This equation together with Eq. (A6) results in

$$\frac{dG_\gamma(V)}{dV}=\frac{1}{\gamma}-\frac{1}{\beta}\frac{G}{I}=0. \tag{A10}$$

Equation (A11) demonstrates that the methods proposed by Werner[6] and Lien *et al.*[11] are equivalent mathematically and only differ from the way to process the data. Werner[6] studied the variation of G/I as a function of G and used all the data of the measured $I(V)$ curve, while Lien *et al.*[11] used only a few data points around the different minima determined by Eq. (A10). These minima correspond to particular values of G/I defined by

$$\frac{G}{I}=\frac{\beta}{\gamma}. \tag{A11}$$

Inserting Eq. (A11) into Eq. (A6), one obtains the following relation between R_s and G:

$$R_sG=\frac{(\gamma-n)}{\gamma}, \tag{A12}$$

which leads to $R_sG=1/2$ in the particular case of the Norde method ($n=1$, $\gamma=2$).

Since

$$\frac{1}{G}=\frac{dV}{dI}=\frac{d(V_d+R_sI)}{dI}=\frac{1}{G_d}+R_s, \tag{A13}$$

Eq. (A12) becomes

$$R_sG_d=\frac{(\gamma-n)}{n} \tag{A14}$$

($R_sG_d=1$ for the particular case of the Norde approach).

Equation (A12) evidences the actual physical significance of the methods proposed by Norde[10] and Lien *et al.*[11] The seeking of the minimum of $G_\gamma(V)$ for each γ value leads to the determination of a data pair (I_0,V_0) of the I-V curve. At this point, the evaluated differential conductance

$G(I_0, V_0) = (\gamma - n)/\gamma(1/R_s)$ simply corresponds to a particular fractional value of the inverse of the series resistance.

[1] S. M. Sze, *Physics of Semiconductor Devices* (Wiley, New York, 1981).
[2] S. S. Cohen and G. Sh. Gildenblat, *Metal–Semiconducteur Contacts and Devices, VLSI Electronics,* edited by N. G. Einspruch (Academic, New York, 1986), Vol. 13.
[3] A. Vapaille and R. Castagné, *Dispositifs et Circuits Intégrés Semiconducteurs* (Dunod, Paris, 1987).
[4] E. H. Rhoderick, *Metal Semiconductor Contacts* (Clarendon, Oxford, 1978).
[5] E. H. Nicollian and A. K. Sinha, *Thin Films—Interdiffusion and Reactions,* edited by J. M. Poate, K. N. Tu, and J. W. Mayer (Wiley, New York 1970), Chap. 13.
[6] J. H. Werner, Appl. Phys. A **47**, 291 (1988).
[7] J. H. Werner and H. H. Gütter, J. Appl. Phys. **69**, 1522 (1991).
[8] D. Donoval, J. de Souza Pires, P. A. Tove, and R. Harman, Solid-State Electron. **32**, 961 (1989).
[9] E. K. Evangelou, L. Papadimitriou, C. A. Dimitriades, and G. E. Giakoumakis, Solid-State Electron. **36**, 1633 (1993).
[10] H. Norde, J. Appl. Phys. **50**, 5052 (1979).
[11] C.-D. Lien, F. C. T. So, and M.-A. Nicolet, IEEE Trans. Electron Devices **ED-31**, 1502 (1984).
[12] K. Sato and D Y. Yasumara, J. Appl. Phys. **58**, 3655 (1985).
[13] J.-C. Manifacier, N. Brortryb, R. Ardebili, and J.-P. Charles, J. Appl. Phys. **64**, 2502 (1988).
[14] K. E. Bohlin, J. Appl. Phys. **60**, 1223 (1986).
[15] R. M. Cibils and R. H. Buitrago, J. Appl. Phys. **58**, 1075 (1985).
[16] T. C. Lee, S. Fung, C. D. Beling, and H. L. Au, J. Appl. Phys. **72**, 4739 (1992).
[17] S. K. Cheung and N. W. Cheung, Appl. Phys. Lett. **49**, 85 (1986).
[18] F. A. Padovani and G. G. Sumner, J. Appl. Phys. **36**, 3744 (1965).
[19] R. Hackan and P. Harrop, IEEE Trans. Electron Devices **ED-19**, 1231 (1972).
[20] M. O. Aboelfotoh, Solid-State Electron. **34**, 51 (1991).
[21] S. Cristoloveanu, Rep. Prog. Phys. **50**, 327 (1987).